Remote Sens. **2009**, *1*, 1380-1394; doi:10.3390/rs1041380

OPEN ACCESS

Remote Sensing

ISSN 2072-4292

www.mdpi.com/journal/remotesensing

Article

Leaf Area Index (LAI) Estimation of Boreal Forest Using Wide Optics Airborne Winter Photos

Terhikki Manninen [1,*], Lauri Korhonen [2], Pekka Voipio [3], Panu Lahtinen [1] and Pauline Stenberg [4]

[1] Finnish Meteorological Institute, P.O. Box 503, FI-00101, Helsinki, Finland; E-Mail: panu.lahtinen@fmi.fi

[2] Faculty of Forest Sciences, P.O. Box 111, University of Joensuu, FI-80101, Joensuu, Finland; E-Mail: lauri.korhonen@uef.fi

[3] Suonenjoki Research Unit, Finnish Forest Research Institute (Metla), Juntintie 154, FI-77600, Finland; E-Mail: pekka.voipio@metla.fi

[4] Department of Forest Resource Management, P.O.Box 27, University of Helsinki, FI-00014, Finland; E-Mail: pauline.Stenberg@helsinki.fi

* Author to whom correspondence should be addressed; E-Mail: terhikki.manninen@fmi.fi; Tel.: +358-9-1929-4159; Fax: +358-9-1929-3146.

Received: 11 November 2009; in revised form: 10 December 2009 / Accepted: 14 December 2009 / Published: 22 December 2009

Abstract: A new simple airborne method based on wide optics camera is developed for leaf area index (LAI) estimation in coniferous forests. The measurements are carried out in winter, when the forest floor is completely snow covered and thus acts as a light background for the hemispherical analysis of the images. The photos are taken automatically and stored on a laptop during the flights. The R^2 value of the linear regression of the airborne and ground based LAI measurements was 0.89.

Keywords: LAI; airborne; hemispherical photo

1. Introduction

The boreal zone land cover has a very significant influence on the northern hemisphere albedo and is an important component of the northern hemisphere carbon budget [1,2]. The boreal forest zone is sensitive to changes in local and global climate [3]. Forest transition zones react to changes in mean temperature and moisture conditions in the long term [4] whereas changes in, for example, forest leaf

area index (LAI) through defoliation indicate stress factors in shorter time scale [5]. Also the timing of the phenological phase transitions is an important indicator of global climatological processes [6].

LAI is one of the Essential Climate Variables (ECV) defined in the Implementation Plan for the Global Observing System for Climate in Support of the United Nations Framework Convention on Climate Change **(**UNFCCC) [7]. Leaf Area Index (LAI) quantifies the amount of leaf material in an ecosystem, and is a measure of the potential of the vegetation of photosynthesis, respiration, rain interception, and other processes that link vegetation to climate. Consequently, LAI appears as a key variable in many models describing vegetation-atmosphere interactions, particularly with respect to the carbon and water cycles [8]. For vegetated land cover, semi-empirical relationships between the surface albedo and LAI are used [9]. The interest in information on LAI distribution and changes has grown substantially in recent decades, due to its importance for climate models and the developing capability for LAI estimation over large areas using satellite measurements. The development and validation of satellite based LAI estimation methods require reliable *in situ* measurements of LAI. For large areas of tall vegetation it is difficult to get aerially representative ground truth using direct or indirect methods [10,11], especially in regions of difficult accessibility.

A new airborne method is presented here for leaf area index estimation. The basic technique is the same as used in hemispherical photo analysis [10,12]. The difference is just that the background is the snow covered terrain instead of the sky. This naturally limits the use of the technique to the areas with annual snow cover. In addition, the method is not directly suited for broadleaved canopies, which are usually without leaves at the time of the snow cover. Boreal forests are typically dominated by coniferous species and the snow covered season is mostly long. Therefore the method is well suited for LAI estimation of boreal forest and especially useful in the northernmost regions, where the roads are sparse and it is difficult to access the forests scattered between wetlands.

2. Experimental Section

2.1. Instrumentation

A normal Canon pocket camera A640 with a 0.7 × wide angle conversion lens WC-D58N (Figure 1) was attached to the helicopter landing gear so that it was looking orthogonally downwards. The angle from the image centre was about 41° at the corners of the rectangular images and 35° and 28° at the middle of the image edges. The images were taken every three seconds and the 3-D GPS coordinates were registered for each image frame. The images were stored in standard jpg format directly to a laptop used for operating the camera. During the flight the last image was repeatedly sent to the screen of the laptop to enable choice of optimal route and altitude. During the flights also another GPS-coordinate recording instrumentation was attached to the helicopter so that two independent GPS-coordinate sets were available.

Figure 1. The camera system attached to the helicopter support landing gear. The arrow points to the hole, through which the camera was mechanically attached.

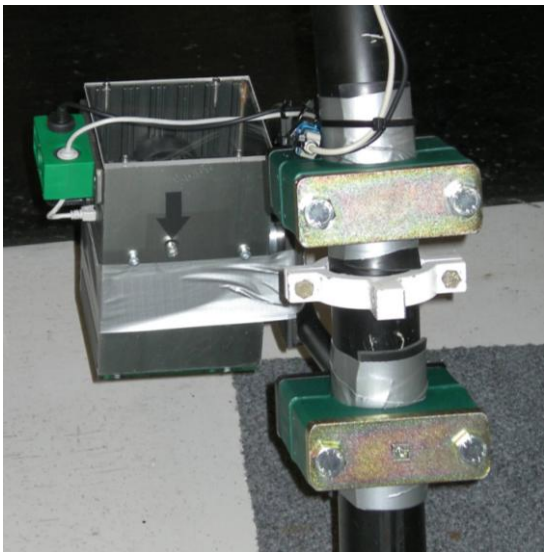

2.2. Flight Plans

The airborne images were acquired in Sodankylä, Finnish Lapland, during the SNORTEX campaign [13]. The reliability of the airborne LAI retrieval method was tested with ground based LAI measurements so that vertical profiles of LAI from tree top level to about 200 m were measured above the ground measurements sites. In 2008 the problem was to exactly locate the profiles while flying, because the helicopter did not have a high accuracy GPS system. In 2009 the exact LAI ground measurement locations were checked on a map before the flights and the helicopter was then directed to the right location visually. Since the flight in March 13, 2009 was carried out in completely overcast situation, there were no shadows at the forest floor. This made the analysis of the photos easy. In March 30, 2008 the weather conditions varied from overcast to partly clear sky, but the photos could still be analyzed with sufficient accuracy. In both cases the difference between the ground and airborne measurement locations could be determined afterwards using the GPS information of the camera system and the GPS coordinates of the ground measurements.

It is not practical to fly at a low altitude for long times. Therefore higher altitude horizontal profiles were flown on a larger area of roughly 100 km × 100 km. The variation of the LAI value range with increasing flight altitude was studied.

2.3. Ground Based LAI Measurements

The LAI field measurements were carried out in the Sodankylä region during July 23–September 13, 2007 and August 26–September 5, 2008 using the Li-Cor LAI-2000 plant canopy analyzer [14] (2007 and 2008) and a camera with a hemispherical lens (2007). The camera lens used for the ground measurements has a full hemispherical view angle, but only zenith angles 0°–75° were utilized in the analysis so as to correspond to measurements by the LAI-2000 instrument which has a maximum zenith angle of 74°. Altogether 68 sample plots were measured in 2007. The plot LAI value was

computed as the mean of 12 LAI-2000 measurements taken below the canopy at ca. 1 m height or of five hemispherical canopy images.

Table 1. The variation range of the location of the ground based measurements in 2007 (individual plots) and 2008 (stand-level).

	2007			2008		
	Minimum	**Maximum**	**Average**	**Minimum**	**Maximum**	**Average**
Latitude (°N)	67.14	67.47	67.35	67.26	67.86	67.50
Longitude (°E)	26.15	27.04	26.66	26.23	27.28	26.69
LAI	0.00	2.78	1.24	0.11	2.22	1.30
Canopy cover (%)	2	78	47	9	86	55
Stand density (stems/ha)	95	17,085	2,332			
Basal area (m2/ha)	0.0	34.0	15.1	1.3	27.8	15.6
Fraction of pine (%)	0	100	59	0	100	61
Fraction of spruce (%)	0	100	23	0	72	21
Fraction of birch (%)	0	83	10	0	57	18
Fraction of other deciduous species (%)	0	22	1	0	3	0.4
Diameter of median tree (cm)	0.0	34.6	16.9	3.4	31.7	19.9
Height of median tree (m)	0.4	24.4	12.2	3.2	21	13.8
Height of the basemedian tree (m)	0.0	11.3	4.5	1.1	10.2	5.2

Because the helicopter directing accuracy was not able to match the location of an individual sample plot well enough, in 2008 the LAI values were derived for stands. Depending on the size of the stand there were 7–22 individual plots within a stand. Some of the stands were so heterogeneous that substands were measured separately. The variation range of the location of the test sites and LAI values and other forestry parameters are given in Table 1. All LAI values used in this study are effective values, *i.e.*, the clumping of the needles is not taken into account. The true LAI values would be about 1.5 times the effective values in Finnish boreal forests [15,16].

2.4. Image Analysis

The airborne wide optics photos and the ground based hemispherical photos were analyzed using MATLAB 7.1 numerical computing environment and programming language (MathWorks Inc. 2008) and image processing toolbox extension. Both ground-based and aerial images were first thresholded using blue component of the RGB image in order to separate the forest canopy from its background (sky or snow). Blue component is ideal for thresholding canopy images, because green vegetation absorbs blue light efficiently, *i.e.*, crowns appear darker. Also the level of background noise is significantly smaller in the blue channel: the brightness difference of blue sky and white clouds is smallest, as well as the influence of shadows in aerial images.

During the flights above our field control sites imaging conditions were perfect, *i.e.*, sky was overcast and no shadows were visible. This was not the case during the second 2009 flight, when the conditions were sunny and shadows clearly visible. The shadows could not be separated from the trees using the same technique as in overcast images, so alternative methods were needed. In earlier studies,

principal component analysis has been utilized to detect shadows from high-resolution winter satellite images [17]. This approach functioned reasonably well also with our data: the second principal component of the RGB image displayed sunlit areas as dark, whereas shadows and trees appeared bright (Figure 2). Thus, most of the shadows could be eliminated by subtracting the (empirically weighted) second principal component from the blue channel, and the result was used as a basis for thresholding (Figure 2). However, the result could not be validated as no field control sites were located at the flight track taken in the sunny day.

Figure 2. Use of principal components in removal of shadows from the images (just a small part of entire image is shown).

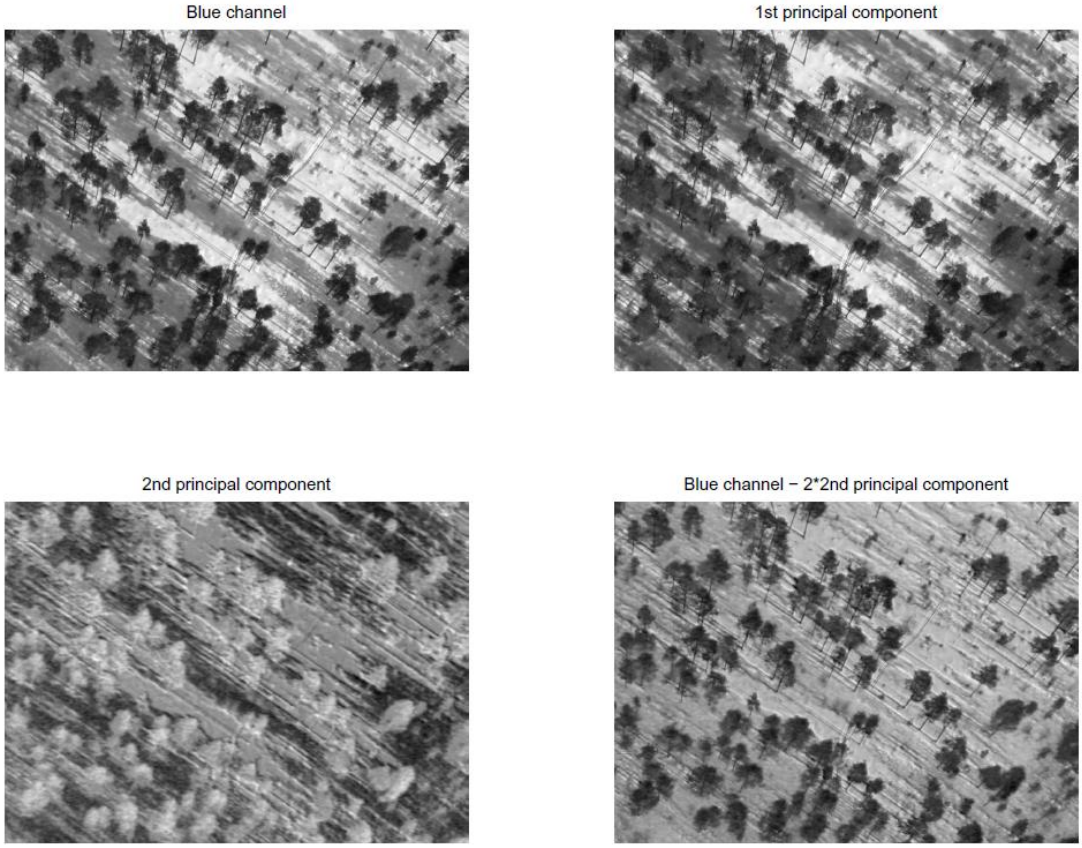

Most of the images were thresholded using the algorithm presented by Nobis and Hunziker [18], which is based on maximizing the brightness difference between the pixels located at the edges of the canopy. However, in some aerial images brightness varied considerably in different parts of the image, which led to situations where the global threshold estimated with Nobis-Hunziker algorithm did not separate canopy pixels well enough from their background. In such cases local thresholding was applied, *i.e.*, different thresholds were determined for different parts of the image. Because our implementation of Nobis-Hunziker algorithm became very slow when applied locally, in these cases the method presented by Ridler and Calvard [19] was used instead. The resultant black-and-white images were saved as 2-bit bitmaps. Finally, the binary aerial images were manually edited to remove non-canopy objects, such as roads and open water, from the images.

Estimation of LAI from binary images is based on transmission of light through the canopy at different zenith angles [10,12]. In theory, following the Beer's law equation, LAI is determined by the integral [12]:

$$LAI = 2\int_0^{\pi/2} -\ln(T(\theta))\cos(\theta)\sin(\theta)d\theta = 2\int_0^{\pi/2} G(\theta)LAI\sin(\theta)d\theta \quad (1)$$

where $T(\theta)$ is the canopy gap fraction at sun zenith angle θ and $G(\theta)$ is the mean projection of unit foliage area.

The estimate of LAI provided by the LAI-2000 instrument is calculated by approximating Miller's integral (Equation 1) with the sum [14]:

$$LAI = 2\sum_{i=1}^{n} -\ln(T_i)\cos(\theta_i)w_i \quad (2)$$

where n (= 5) is the number of concentric rings for which gap fraction T_i is measured, θ_i is the mean zenith angle of ring i, and w_i is weight for the specified ring, calculated with Equation 3:

$$w_i = \frac{\sin(\theta_i)}{\sum_{j=1}^{n}\sin(\theta_j)} \quad (3)$$

Hemispherical *in situ* images were analyzed using a similar method: the binary image was divided into five concentric rings (0–15°,…, 60–75°), which are approximately the same as those of the LAI-2000. Following the LAI-2000 methodology, zenith angles 75–90° were not utilized (a difference to Miller [12]), but ring 60–75° was weighted as if it covered the entire range 60–90° [14]. The same procedure was however not applicable to the aerial images because the maximum nadir angle viewed by the aerial camera was considerably smaller (horizontal 35.1°, vertical 27.5°). Instead, the aerial images were divided into four concentric rings, having a width of 10° each. Canopy gap fractions were calculated from the binary images as the proportion of white background pixels within each ring, and LAI was estimated using Equation 2.

Equation 1 (Miller's integral) is based on that averaging $G(\theta)$ (= $lnT(\theta)cos(\theta)/LAI$) over all view directions (zenith angles from 0° to 90°) yields the value G_{mean} = 0.5, irrespective of the foliage angle distribution. When integration is performed over a narrower range of zenith angles, this does not exactly hold true (except for a spherical foliage angle distribution) and LAI (calculated from Equation 2) will be underestimated if $G_{mean} < 0.5$ and overestimated if $G_{mean} > 0.5$. The potential bias is larger the smaller is the zenith angle range (over which G is averaged) and, thus, the aerial LAI estimates must be considered less precise than the ground based estimates (from hemispherical photos or LAI-2000).

The image analysis chain used for hemispherical *in-situ* images was validated by comparing the results to LAI-2000 readings obtained simultaneously from the same locations. Because the two thresholding methods produced systematically different threshold values, the thresholds produced by the algorithms were adjusted by adding a constant that minimized the bias in LAI when compared to LAI-2000. For Nobis-Hunziker algorithm this threshold-fix was −7 and for Ridler-Calvard +20 (the scale of 8-bit blue channel is 0–255). After the adjustment both methods showed a 1:1 relationship

with LAI-2000 data (Figure 3). There was one outlier caused by a dark cloud in the Nobis-Hunziker plot (Figure 3), but in practice such images can be observed and removed from the analysis.

Figure 3. Image thresholding methods validated with LAI-2000 data.

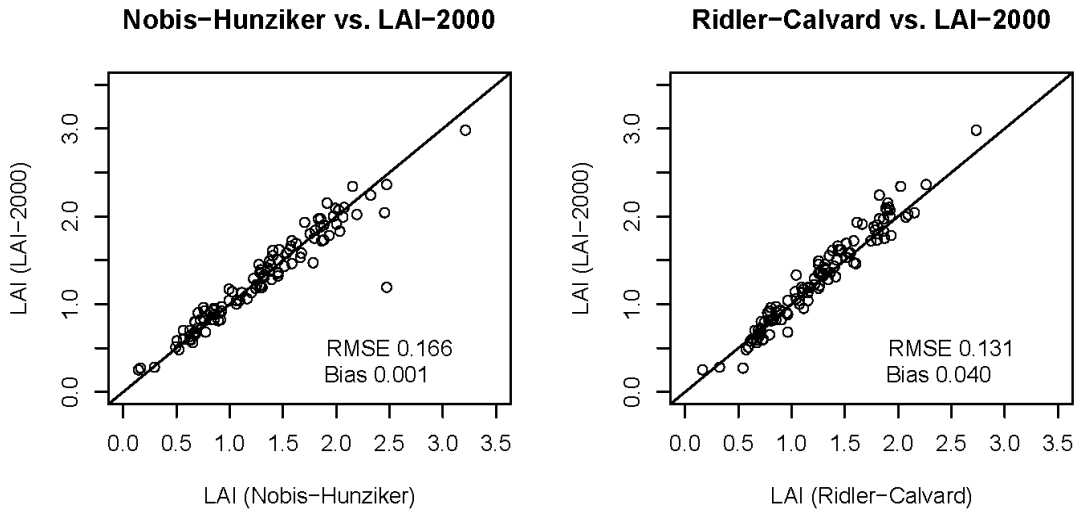

An example of the variation of the area included in the photos of one vertical profile from the lowest to the highest altitude is shown in Figure 4. Corresponding thresholded binary images are shown as well. An example of the resolution of the camera is shown in Figure 5. The LAI profile calculated from the series of images of the profile of Figure 4 is shown in Figure 6.

Figure 4. Example of photos of one vertical profile taken at Kommattivaara (67.440° N, 26.745° E) in March 13, 2009 using the wide optics airborne camera. (a) Altitude above ground about 25 m, (b) altitude above ground about 210 m. The corresponding thresholded binary images are shown below.

Figure 4. *Cont.*

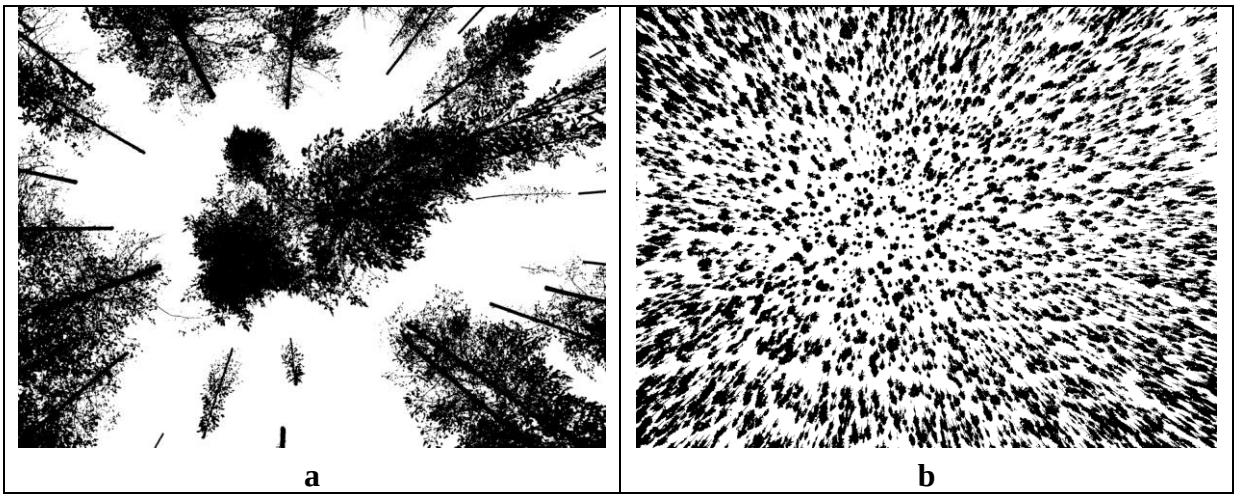

Figure 5. A detail of image (a) in **Figure 4** demonstrating the resolution of the camera.

Figure 6. The airborne LAI profile corresponding to Figure 4.

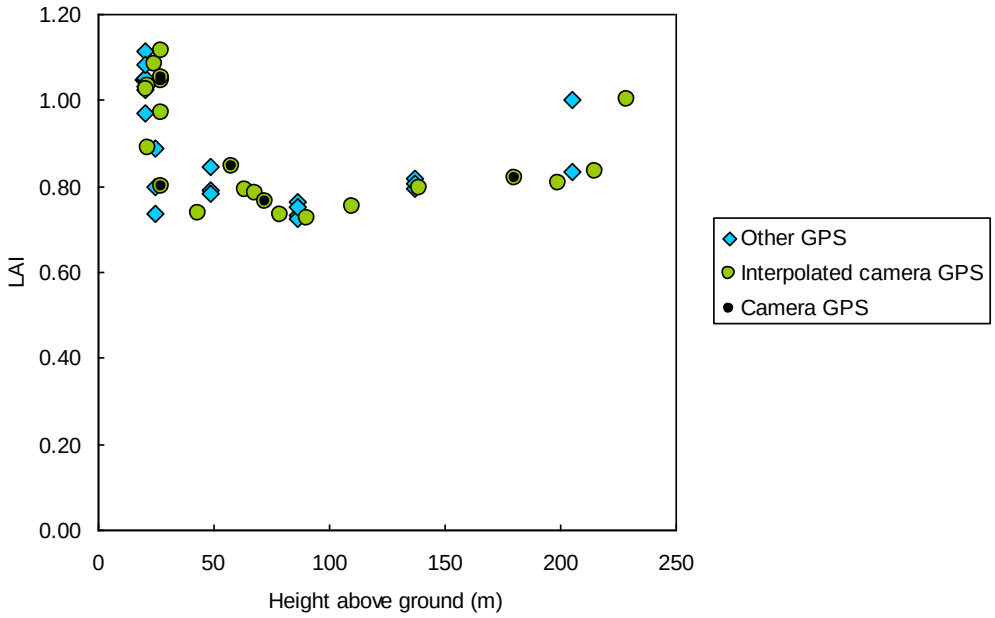

3. Results and Discussion

Variation in LAI for different vertical profiles was mainly due to the heterogeneous structure of the forests. When a dense forest patch was surrounded by open areas, LAI decreased with increasing flight altitude, whereas the opposite behaviour was observed when a sparse clearing in a forest was at the centre of the image. Thus it is not trivial, from which altitude the LAI value should be taken to compare with the ground measurements. The forest area detected by the ground based and airborne measurements should be about the same. For LAI-2000 the largest zenith angle is 74°, so that the radius of the area would be about 3.4 times the canopy height. In the Sodankylä region the average tree height measured in 2008 was 13.8 m and the minimum and maximum values 3.2 m and 21 m, respectively. The hemispherical lens has even wider view angle, but the pixels corresponding to the largest view angles were ignored, so that approximately the same area was detected by the hemispherical camera as the LAI-2000 instrument [20]. To detect the same area with the smaller viewing angle (41°) of the airborne system, the observation height should be about tan(74°)/tan(41°) = 4 times the tree height, which varied in the test area from 13 m to 84 m with an average value of 55 m (Table 1).

Figure 7. The relationship of the canopy height and the average altitude of the two GPS systems corresponding to the images to be used for LAI retrieval comparison with ground measurements. The missing GPS height values of the camera system were interpolated before taking the average of the two GPS systems. The terrain height was subtracted from the GPS height values. The GPS heights of the two systems are shown as error bars of the average value. The outlier (blue marker) not included in the regression corresponds to a plot, which was so close to the road, that the LAI values derived from the higher altitudes were deteriorated by that.

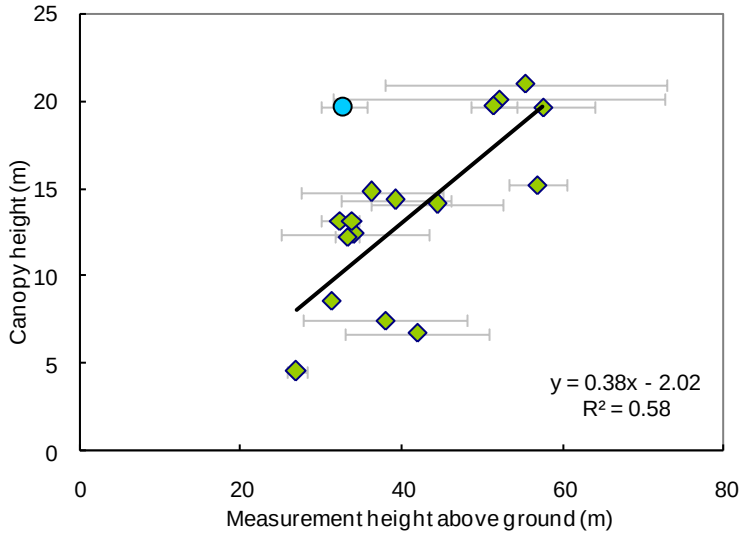

The two independent GPS-coordinate data sets were compared and it turned out that the latitude and longitude values were equal with a high precision. The height values, on the contrary, varied on the average 8.4 m with a standard deviation of 9.5 m during the whole flight (which contained 624 height value pairs) although the general trend was the same ($R^2 = 0.96$). This was due to the different logic of

the two measurement systems. The GPS of the camera produced an instantaneous height value on the average for every 12 seconds (*i.e.*, for every 4th image), whereas the other GPS provided an average height coordinate value every 10 seconds. The absolute accuracy of the vertical profile heights is not good enough to be used for choosing the image for LAI comparison with ground measurements. Yet the optimal height should increase with increasing canopy height. Therefore all altitudes were also roughly checked by visual inspection of the photos. The GPS heights were given with respect to sea level and the terrain heights obtained from a digital elevation model of 10 m resolution were subtracted from the GPS heights to obtain flight altitudes with respect to the ground. The altitudes of the chosen images were compared to the canopy height values (Figure 7).

The LAI values derived from the airborne wide optics photos were compared to the stand wise average LAI values obtained from the hemispherical photos taken in the same locations in the previous autumn. In coniferous forest the difference between the leaf area index in summer and winter conditions is not large. For two plots with no deciduous trees the LAI values measured at ground in winter 2008 and in summer 2008 differed only 0.02 and −0.24, although it was not possible to achieve exactly identical geolocation. The comparison results are shown in Figure 8.

Figure 8. Relationship of the ground based and airborne LAI values. The airborne values were measured in March 13, 2009 and corresponding ground measurements were carried out during August 26–September 5, 2008 The points for airborne measurements 2008 and ground measurements 2007, for which the airborne location is closer than 30 m to that of the ground measurements and which don't have deciduous LAI contribution, are shown as well.

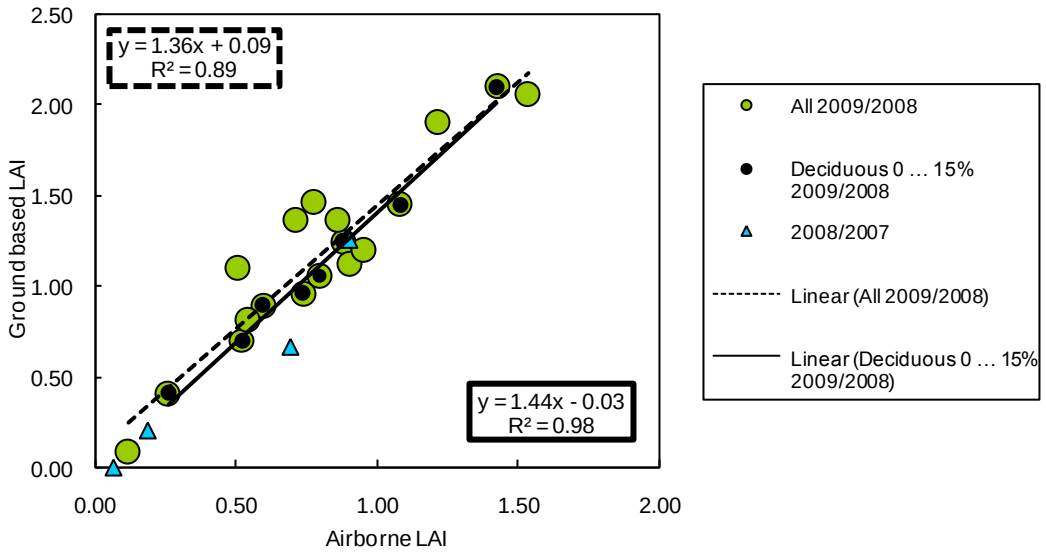

The coefficient of determination of the linear regression between the LAI values by the two methods is high (R^2 = 0.89 for all stands and R^2 = 0.98 for coniferous stands) and the offset small. The standard error for the predicted LAI using the airborne LAI was 0.12 for all data and 0.05 for stands with less or equal to 15% deciduous species. However, the slope of the regression lines significantly deviates from unity: the ground based ("true") LAI was on average 36% (44%) higher than the airborne LAI. The bias in the airborne LAI is explained by the limited zenith angle range of the aerial photos. More precisely, a value of G_{mean} = 0.37 (instead of 0.5) for the aerial photos would cause the

LAI estimate to differ from its true value by the observed amount. *G*-values calculated from the ground based hemispherical photos are shown in Figure 9. At the smallest zenith angle of 7 degrees (corresponding to the mean angle of the uppermost ring of the LAI-2000 instrument), the value of *G* averaged 0.4 (excluding the single outlier, a sapling stand), and was dominantly closer to 0.4 than 0.5 throughout the zenith angle range corresponding to that of the aerial photos. Subsequently, when the hemispherical photos (ground data of 2007) were analyzed using only the zenith angle range of the airborne data, the ratio of LAI derived using the full zenith angle range to LAI derived using the smaller zenith angle range was similar to the slope(s) of the regression lines in Figure 8. For all data, the ratio was on average 1.38 with a standard deviation of 0.55. The ratio for the ground based LAI values (derived using a wide angle range) to the airborne LAI values for 2008/2009 (derived using the small angle range) was on the average 1.47 with a standard deviation of 0.31. When only stands with deciduous contribution up to 15 % were analyzed the ratio was 1.41 with a standard deviation of 0.09.

Figure 9. Standwise values of the mean projection of unit foliage area (G) as a function of sun zenith angle, calculated from ground based hemispherical photos of 2008.

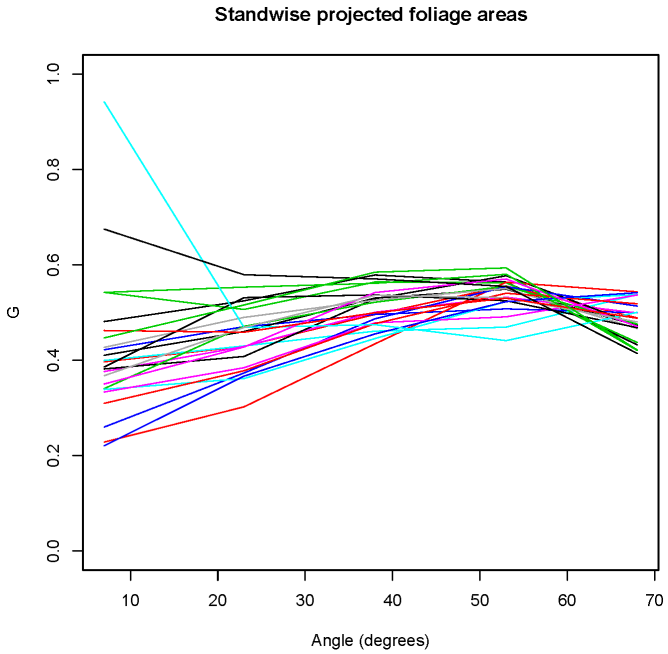

In addition, even if the cross sectional area of the canopy covered by the airborne and ground based photos were equal the part of the canopy detected would not be equal due to the conical viewing geometry (when fully hemispherical viewing is not applied). The airborne photos will then contain at the edges only lower parts of the trees, whereas the ground based photos will see only the top part of the same trees. Therefore the airborne LAI estimate inevitably tends to be slightly smaller than the ground based estimate, especially for Scots pine, the crown of which can be located altogether very high up.

Taking into account that the LAI correlation of two different ground based methods (LAI-2000 and hemispherical photos) had a root mean square error of 0.131…0.166 (Figure 3), the difference between the airborne and ground based LAI value is of the order of the measurement method accuracy of hemispherical photos. Judging from that the coefficient of determination of the relationship between

ground based and airborne LAI for purely coniferous stands is very high (Figure 9), the effect of the decreased zenith angle range is the same for all canopies in the studied area, *i.e.*, they have similar *G*-values in the zenith angle range covered by the aerial photos. If this turns out to be more generally true, the linear coefficient has to be calibrated empirically once, but then it can be used for the same kind of forests as long as the airborne camera system remains the same.

When the regression line of Figure 8 comprising all data points was applied to the airborne data (to scale them to the level of the ground data), the average difference between the LAI values of the two data sets was 0.14 for the whole data and 0.06 for stands with up to 15% deciduous trees. The three obvious airborne LAI underestimates seen in Figure 8 were obtained in stands with a larger fraction of deciduous trees among the coniferous species, which naturally decreases the LAI value in winter (airborne) from that obtained in the autumn (ground based) (Figure 10). The results of 2008/2007 are deteriorated due to the mismatch of the location of the airborne and ground based measurements, which was obvious also from the images.

Figure 10. LAI is underestimated in forests with large percentage of deciduous trees.

The measured LAI values depend on the flight altitude. The lower the altitude is the smaller is the area seen by the camera and the larger is the variation of diverse scenes, whereas high altitude flights produce more averaged LAI values. The range of variation in LAI with varying flight altitude is shown in Figure 11 for all points acquired March 13, 2009. The data contains the vertical profiles and the horizontal flights between the successive profile locations. Obviously the maximum LAI value decreases markedly when the flight altitude increases from the tree tops to about 100 m. There is no single optimal flight altitude to derive LAI estimates. If one is interested in characterizing small forest stands, the flight altitude should be chosen so that the image area matches about that of typical ground measurements. On the other hand, if one is interested in comparing the values with satellite based LAI estimates it might be more useful to cover the area of a satellite pixel, so that both instruments would directly measure the same target area. However, one has to take into account that the resolution decreases with increasing flight altitude, so that the detection of gaps inside crowns may not be possible after some critical altitude. Further studies and comparison with satellite based LAI estimates are needed to find the optimal flight altitude range.

Figure 11. The observed LAI value versus the flight altitude above ground in March 13, 2009. The values are scaled using the regression line of Figure 8 for all data points of 2009.

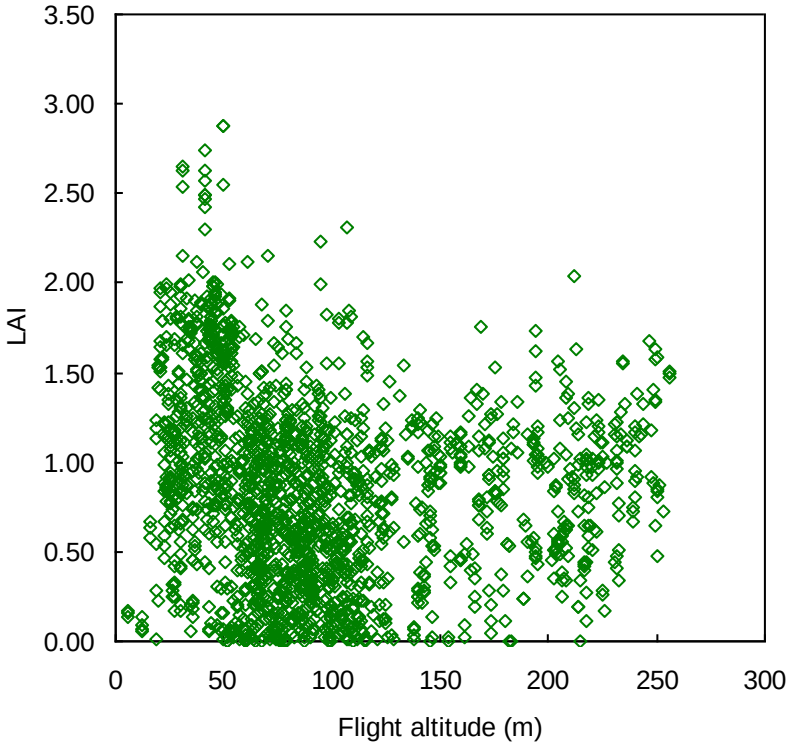

The derived LAI retrieval method is well suited to areas with difficult accessibility at ground level. Cloudy weather is better than sunny, because then there are no obvious shadows at the forest floor. However, the shadows can be removed using the principal component analysis (Figure 2) [17]. The snow cover at the forest floor makes a good background, but no snow on the trees can be accepted.

4. Conclusions

The airborne wide optics technique presented here has been shown to be applicable for LAI estimation in the boreal zone in winter time. The achievable accuracy of the obtained LAI estimates seems to be comparable to that of the ground measurements. The derived method suits for LAI measurements in large areas and especially well in areas which are difficult to access. One alternative for reducing costs is to use UAV (unmanned aerial vehicle) platforms instead of a helicopter, as many UAVs can carry lightweight cameras well suited for obtaining this kind of simple aerial images. They can also fly safely at low altitudes. Their drawback is the need for relatively calm weather.

Clear need for further studies is in the analysis of this kind of imagery. Waiting for overcast flight conditions may not be always possible, although the boreal zone winters are dominantly cloud covered, so methods for processing images gathered in clear sky conditions must be developed. The main problem in sunny images is the effect of shadows. The shadow detection method based on principal components analysis that we tested functioned reasonably well, but other methods based on spectral and directional properties of shadows could function better. Automatic removal of other dark non-canopy objects, such as roads or open water, should also be possible based on spectral properties of green vegetation. In this study such objects were removed manually from the binary images, but if

the number of images is large and frequency of such objects is high, this may become too laborious. The basis for an improved method should still be that the trees are classified correctly in all illumination conditions, as it is much easier to remove extra objects during the binary image check than add missing trees.

Acknowledgements

The authors are grateful to Mikko Viitapohja from Vogon IT for construction of the camera system and Eero Rinne for technical support in using it in 2008. Heliflite Oy is acknowledged for carrying out the helicopter flights. The work was financially supported by EUMETSAT through the joint activity funding of the Climate-SAF and LSA-SAF projects in the SNORTEX campaign, and the Finnish Graduate School of Forest Sciences (GSForest).

References and Notes

1. Bonan, G.B.; Pollard, D.; Thompson, S.L. Effects of boreal forest vegetation on global climate. *Nature* **1992**, *359*, 716-718.
2. Randerson, J.T.; Liu, H.; Flanner, M.G.; Chambers, S.D.; Jin, Y.; Hess, P.G.; Pfister, G.; Mack, M.C.; Treseder, K.K.; Welp, L.R.; Chapin, F.S.; Harden, J.W.; Goulden, M.L.; Lyons, E.; Neff, J.C.; Schuur, E.A. G.; Zender, C.S. The Impact of Boreal Forest Fire on Climate Warming. *Science* **2006**, *314*, 1130-1132.
3. Parry, M.L.; Canziani, O.F.; Palutikof, J.P.; van der Linden, P.J.; Hanson, C.E. IPCC: *Climate Change 2007: Impacts, Adaptation and Vulnerability. Contribution of Working Group II to the Fourth Assessment Report of the Intergovernmental Panel on Climate Change*; Cambridge University Press: Cambridge, London, UK, 2007; p. 976.
4. Solantie, R. Productivity of boreal forests in relation to climate and vegetation zones. *Boreal Environ. Res.* **2005**, *10*, 275-297.
5. ICP Forests. *The Condition of Forests in Europe, 2007 Executive Report*, Federal Research Centre for Forestry and Forest Products (BFH): Hamburg, Germany and Brussels, Belgium, 2007, p. 33.
6. Menzel, A.; Sparks, T.H.; Estrella, N.; Koch, E.; Aasa, A.; Ahas, R.; Alm-Kübler, K.; Bissolli, P.; Braslavská, O.; Briede, A.; Chmielewski, F.M.; Crepinsek, Z.; Curnel, Y.; Dahl, Å.; Defila, C.; Donnelly, A.; Filella, Y.; Jatczak, K.; Måge, F.; Mestre, A.; Nordli, Ø.; Peñuelas, J.; Pirinen, P.; Remiřová, V.; Scheifinger, H.; Striz, M.; Susnik, A.; Van Vliet, A.J.H.; Wielgolaski, F.-E.; Zach, S.; Zust, A. European phenological response to climate change matches the warming pattern, Glob. Change Biol. **2006**, *12*, 1969-1976.
7. *The second report on the adequacy of the global observing systems for climate in support of the UNFCCC, GCOS-82, WMO/TD No. 1143*; United Nations Environment Programme; International Council for Science, World Meteorological Organization: Geneva, Switzerland, 2003, p. 74
8. Gobron, N.; Verstraete, M.M. *ECV 11: Assessment of the Status of the Development of Standards for the Terrestrial Essential Climate Variables*; GTOS 66: Rome, Italy, November, 2009.
9. Roujean, J.-L.; Leroy, M.; Deschamps, P.-Y. A Bidirectional Reflectance Model of the Earth's Surface for the Correction of Remote Sensing Data. *J. Geo. Res.* **1992**, *97*, 20455-20468.

10. Jonckheere, I.; Fleck, S.; Nackaerts, K.; Muysa, B.; Coppin, P.; Weiss, M.; Baret, F. Review of methods for in situ leaf area index determination Part I. Theories, sensors and hemispherical photography. *Agri. For. Meteo.* **2004**, *121*, 19-35.
11. Breda, N.J. Ground-based measurements of leaf area index: a review of methods, instruments and current controversies. *J. Exp. Bot.* **2003**, *54*, 2403-2417.
12. Miller, J.B. A formula for average foliage density. *Aust. J. Bot.* **1967**, *15*, 141-144.
13. Roujean, J.-L.; Manninen, T.; Kontu, A.; Peltoniemi, J.; Hautecoeur, O.; Riihelä, A.; Lahtinen, P.; Siljamo, N.; Lötjönen, M.; Suokanerva, H.; Sukuvaara, T.; Kaasalainen, S.; Aulamo, O.; Aaltonen, V. Thölix, L.; Karhu, J.; Suomalainen, J.; Hakala, T.; SNORTEX (SNOw Reflectance Transition EXperiment): Remote Sensing measurement of the dynamic properties of the boreal snow-forest in support to climate and weather forecast: Report of IOP-2008. In *Proceedings of IGARSS'09*, Cape Town, South Africa, 2009, in press.
14. *LAI Plant Canopy Analyzer*, *Instruction Manual*. LI-COR: Lincoln, NE, USA, 1992.
15. Stenberg, P.; Nilson, T.; Smolander, H.; Voipio, P. Gap fraction based estimation of LAI in Scots pine stands subjected to experimental removal of branches and stems. *Can. J. Remote Sens.* **2003**, *29*, 363-370.
16. Stenberg, P.; Rautiainen, M.; Manninen, T.; Voipio, P. Boreal forest leaf area index from optical satellite images: model simulations and empirical analyses using data from central Finland. *Boreal Environ. Res.* **2008**, *13*, 433-443.
17. Peterson, U.; Liira, J.; Mander, Ü. *Edge Proximity Influence on Radiance at Forest Edges on a very High Resolution IKONOS Winter Satellite Image*; Nordic Remote Sensing Days: Helsinki, Finland, 2009.
18. Nobis, M.; Hunziker, U. Automatic thresholding for hemispherical canopy-photographs based on edge detection. *Agr. For. Meteo.* **2005**, *128*, 243-250.
19. Ridler, T.W.; Calvard, S. Picture thresholding using an iterative selection method. *IEEE Trans. Syst. Man Cybern.* **1978**, *8*, 630-632.
20. Rautiainen, M.; Suomalainen, J.; Mõttus, M.; Stenberg, P.; Voipio, P.; Peltoniemi, J.; Manninen, T. Coupling forest canopy and understory reflectance in the Arctic latitudes of Finland. *Remote Sens. Environ.* **2007**, *111*, 332-343.